

Thin-SOI Digital Accelerometer Employing Pull-in Time Mode Configuration

L. Pakula, V. Rajaraman and P.J. French

Abstract—We aim to present the principle, design, fabrication and measurement results of a quasi digital accelerometer fabricated on thin silicon-on-insulator (SOI) substrate. The presented device features quasi-digital output, therefore eliminating the need for analogue signal conditioning. The accelerometer can be directly interfaced to digital electronic circuitry. The measurements showed a pull-in voltage of 2.7V and a pull-in time from 0 to 1G to be 3.2 μ s.

Index Terms—Pull-in mode, thin-SOI, accelerometer

I. INTRODUCTION

AMONG a range of silicon micromachining technologies, micromachining on thin-SOI substrate provides a good platform for monolithic integration of MEMS devices with the IC readout circuitry. Moreover, thin-SOI micromachining technology enables chip-scale packaging of small footprint MEMS devices on wafer-level, by sealing the MEMS devices with additional deposited layers. On the other hand, large footprint MEMS structures can readily be packaged using wafer bonding techniques. Hence, thin-SOI micromachining technology can be effectively leveraged to realise low-cost accelerometers for automotive, consumer and medical applications.

It is known that the pull-in voltage and pull-in time are functions of the applied acceleration [1, 2]. In this work, a quasi-digital accelerometer with pull-in time-mode configuration [2] has been fabricated on thin-SOI substrate with its sensitive axis in the wafer plane.

II. PRINCIPLE

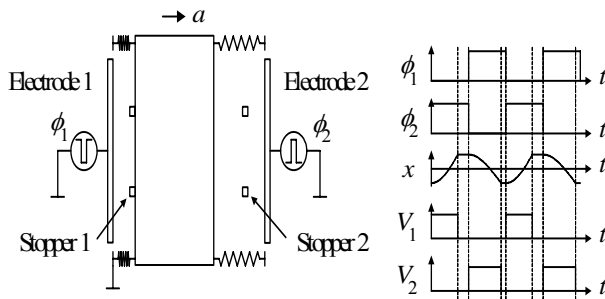


Fig. 1. The principle of the pull-in operation mode

The principle of the device is shown in Fig. 1. By applying the pulse voltages ϕ_1 and ϕ_2 to the electrodes 1 and 2 alternately, the mass is pull-in at the stoppers 1 and 2 alternately. T_1 is the pull-in time from the stopper 1 to 2, and T_2 is pull-in time from the stopper 2 to 1. When there is no

acceleration in the x direction, $T_1=T_2=T_0$. If there is an acceleration in the x direction, the differential pull-in time, $\Delta T=T_2-T_1$, is proportional to the acceleration. ΔT is a pulse-width-modulated signal and can be measured with a digital circuit. The sensitivity and the non-linearity are similar to that of the differential capacitive sensing.

III. ANALYSIS

Asdasd The movement of the mass between the stoppers can be described by the equation:

$$m\ddot{x} + c\dot{x} + kx = \frac{\epsilon\epsilon_0AV^2}{2(d_0 - x)^2} + ma \quad (1)$$

where a is the acceleration, V the driving voltage, A the area of the electrode, d_0 the initial electrode gap and x the displacement. To keep the device working in the pull-in mode, the driving voltage must be higher than the minimum pull-in voltage and the previous pulse voltage should be held long enough to make sure that the initial condition is $\dot{x}=0$. To discuss the characteristics in general, a dimensionless equation is preferred. The corresponding dimensionless equation of (1) is

$$\ddot{\tilde{x}} + 2\zeta\dot{\tilde{x}} + \tilde{x} = \frac{\tilde{F}}{(1-\tilde{x})^2} + \tilde{a} \quad (2)$$

where $\tilde{x} = x/d_0$, $\dot{\tilde{x}} = d\tilde{x}/d\tau$, $\ddot{\tilde{x}} = d^2\tilde{x}/d\tau^2$, $\tau = \omega_0 t$, ω_0 the circular resonant frequency, ζ the damping ratio, $\tilde{F} = \epsilon\epsilon_0AV^2/(2kd_0^3)$ the dimensionless driving force and $\tilde{a} = ma/kd_0$ the dimensionless acceleration. The driving force must fulfil $\tilde{F} > 4/27$, which is corresponding to the minimum pull-in voltage. \tilde{a} is always smaller than 1 according to the definition.

When the damping is zero, the analytical pull-in time can be obtained [2]. The differential pull-in time $\Delta\tau = \tau_2 - \tau_1$ is

$$\Delta\tau = 2s\tilde{a} + \frac{17}{4}n\tilde{a}^3 + o(\tilde{a}^3) \quad (3)$$

where

$$s = \int_{-\lambda}^{\lambda} (\lambda + \tilde{x})^{-\frac{1}{2}} \left((\lambda - \tilde{x}) + \frac{2\tilde{F}}{(1-\tilde{x})(1+\lambda)} \right)^{-\frac{3}{2}} d\tilde{x} \quad (4)$$

$$n = \int_{-\lambda}^{\lambda} (\lambda + \tilde{x})^{-\frac{1}{2}} \left((\lambda - \tilde{x}) + \frac{2\tilde{F}}{(1 - \tilde{x})(1 + \lambda)} \right)^{\frac{7}{2}} d\tilde{x} \quad (5)$$

where, $\pm\lambda$ is the positions of the stoppers.

It can be obtained from (3) that $\Delta\tau$ is proportional to the acceleration. The gain of the device can be defined as $G = 2s/\tau_0$. Fig. 2 shows the gain with respect to \tilde{F} and λ . By comparison, the gain of the differential capacitive sensing is 2. Therefore, the gain of the pull-in accelerometer is comparable to that of the normal accelerometer with the differential capacitive sensing.

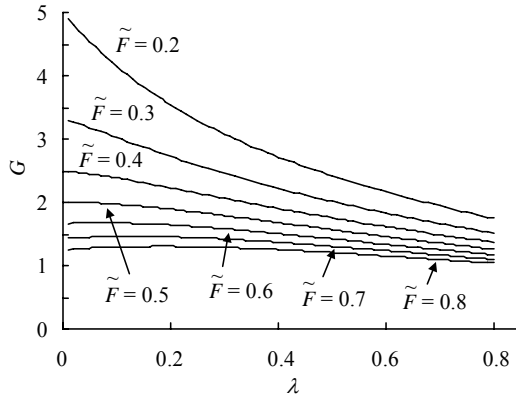


Figure 2. The gain as the function of \tilde{F} and λ

The nonlinearity of the pull-in accelerometer is $O(\tilde{a}^3)$, which is the same order of the ratio $(17/4)n\tilde{a}^3/(2s\tilde{a})$. The nonlinearity of the pull-in mode is similar to the differential capacitive sensing.

When the damping is non zero but also not high, (2) cannot be solved analytically. Matlab was used to analyse the equation numerically. Fig. 3 shows the gain with respect to the electrostatic force and Fig. 4 the nonlinearity in the range of $\tilde{a} \in [-0.1, 0.1]$. λ used in the calculations is 0.5.

It can be observed that both the gain and the nonlinearity increase with the damping and saturate when the damping ratio is larger than 1.

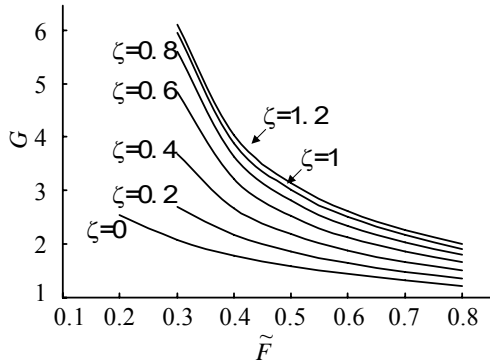


Figure 3. The gain as the function of \tilde{F} and ζ . λ is supposed to be 0.5.

As the damping in an accelerometer is usually changed

with the displacement, the influence of the variable damping is also analysed. The dominant damping in the system is supposed to be the squeeze film damping, which means that the damping ratio is inversely proportional to the cube of the electrode gap. It is observed that the gain increases with the damping faster than in Fig. 3.

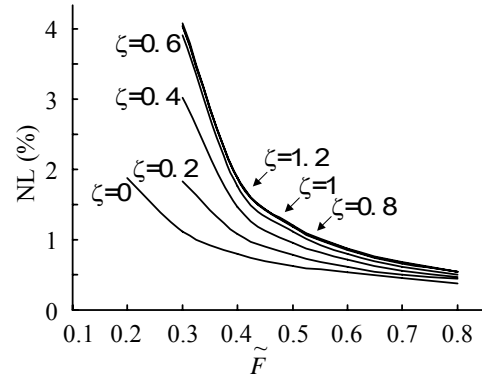


Figure 4. Nonlinearity as the function of \tilde{F} and ζ . λ is supposed to be 0.5

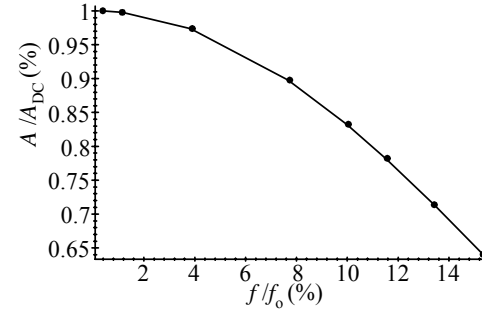


Figure 5. The amplitude-frequency relation

The pull-in operation process is a pulse-width modulation process [3]. The bandwidth of the device is determined by the sampling rate. In principle, the larger the sampling rate, the larger the bandwidth. The theoretical maximum sampling rate of the pull-in accelerometer is a higher than the resonant frequency. However, the sampling rate is limited by several factors.

Firstly, the sampling pulse width must be larger than the maximum pull-in time, which is determined by the full-scale required. Secondly, the sampling pulse width must be long enough to make sure that the speed of the mass is 0 before the next pulse because the measurement is sensitive to the initial conditions and the vibration of the mass at the pull-in position causes errors. In this paper, the pulse width of the driving voltage is set to be $1/f_0$, where f_0 is the resonant frequency. A full measuring circle is $2/f_0$. In other words, the sampling frequency is $f_0/2$.

Fig. 5 shows the amplitude-frequency relation of a device with $\zeta=0$, $\lambda=0.5$ and $\tilde{F}=0.3$. The relation is obtained by Fourier transform of the theoretical output. The bandwidth of the device is 13.4% of the resonant frequency.

When the acceleration is very large, the structure does not

pull-in. The maximum acceleration that can be measured is a function of the operating voltage. To simplify the analysis, the maximum acceleration is estimated with the initial conditions $\tilde{x} = 0$ and $\tilde{\dot{x}} = 0$.

When the damping is very high, the maximum acceleration is:

$$|\tilde{a}| < \sqrt[3]{\frac{27\tilde{F}}{4}} - 1 \quad (6)$$

For the device with light damping, the maximum acceleration is larger than (6) due to over-shooting [1]. The maximum acceleration of the device without damping is given by:

$$|\tilde{a}| = \sqrt{2\tilde{F}} - \frac{1}{2} \quad (7)$$

IV. DESIGN

Based on the above analysis the surface micromachined accelerometer has been design. The device structure is made by $4\mu\text{m}$ thick silicon. The mass is supported by four folded beams. The mass is $400\mu\text{m} \times 800\mu\text{m}$. Each fold of the beam is $2.5\mu\text{m} \times 150\mu\text{m}$. Interdigitated electrodes are used to drive the mass. There are 62 fingers on each side of the mass. Each finger is $3\mu\text{m} \times 100\mu\text{m}$. The finger-electrode gap is $2\mu\text{m}$. The mass-stopper gap is $1\mu\text{m}$. The mass-substrate gap is 400nm . The electrical and mechanical properties have been calculated and presented in Table 1. The resonant frequency is calculated to be 1.8 kHz . When the displacement is 0, the damping ratio is calculated to be 0.104. The pull-in voltage is calculated to be 2.88V . The pull-in voltage of fingers is higher than 10V when the mass is at the pull-in position. The static and dynamic properties of the accelerometer in pull-in mode are analysed numerically with Matlab software. When the driving voltage is 8V , the pull-in time is calculated to be $77\mu\text{s}$. Fig. 6 shows the differential pull-in time with respect to the acceleration, which was obtained by simulation. The non-linearity is $0.87\% \text{FS}$.

Table 1. Mechanical and Electrical Device Parameters

Resonance Frequency	1810 Hz
Pull-in Voltage	2.36 V
Rest Capacitance	165 fF
Thermal Noise	11.2 $\mu\text{g}/\sqrt{\text{Hz}}$
Sensitivity	3.2 $\mu\text{s}/\text{g}$

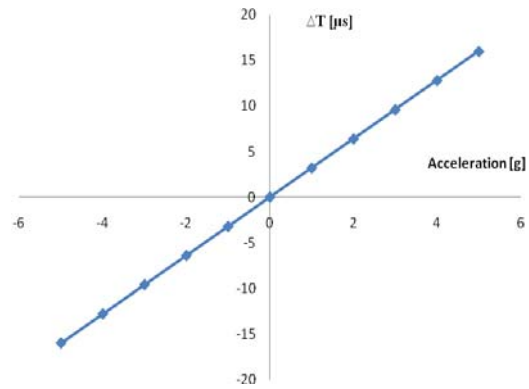


Figure 6. Pull-in time vs. acceleration

V. FABRICATION PROCESS

The post-IC fabrication process illustrated in Fig. 7 uses a single-mask and a 100mm , $400\mu\text{m}$ thick SOI substrate as the starting material (Fig. 7.1). The active silicon layer is $4\mu\text{m}$ thick and the buried oxide thickness is 400nm . The initial step starts with the deposition of photoresist mask followed by lithographic patterning of the microaccelerometer structure (Fig. 7.2). The active silicon layer is patterned using RIE, stopping on the buried oxide (Fig. 7.3). The buried oxide layer is then sacrificially etched using a HF-based etchant to release the microstructure (Fig. 7.4). This step is immediately followed by a Cyclohexane-based freeze-drying process in order to avoid stiction of the released microstructures. Finally, a thin layer of aluminium is sputtered onto the bond pads, completing the device processing (Fig. 7.5).

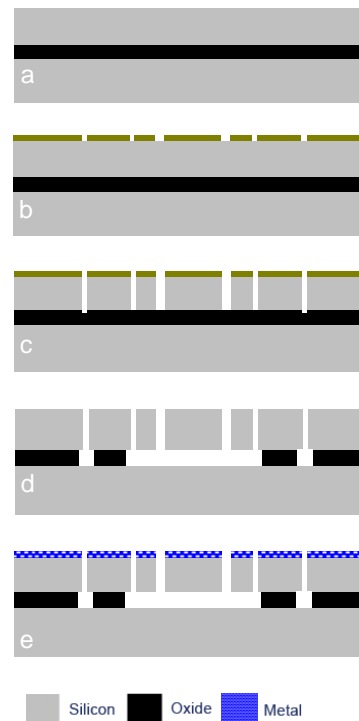


Figure 7. Thin-SOI MEMS Fabrication Process

VI. RESULTS

Figs. 8 and 9 show the released microstructure of the quasi-digital accelerometer.

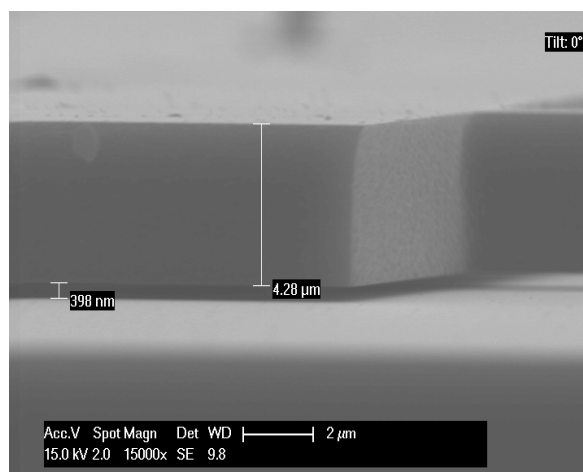


Figure 8. SEM image of a freestanding thin-SOI layer

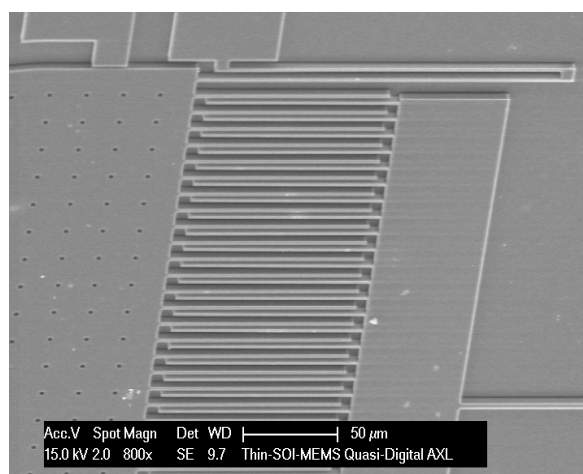


Figure 9. SEM image of the quasi-digital accelerometer

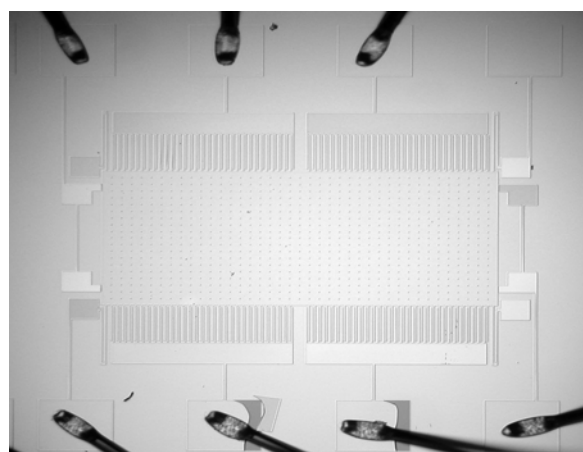


Figure 10. Photo of the quasi-digital accelerometer

Fig. 10 presents top view of fabricated device which was measured. The capacitance-voltage results are shown in Fig. 11. The pull-in voltage was around 2.7 V which can be explained due to the process variation.

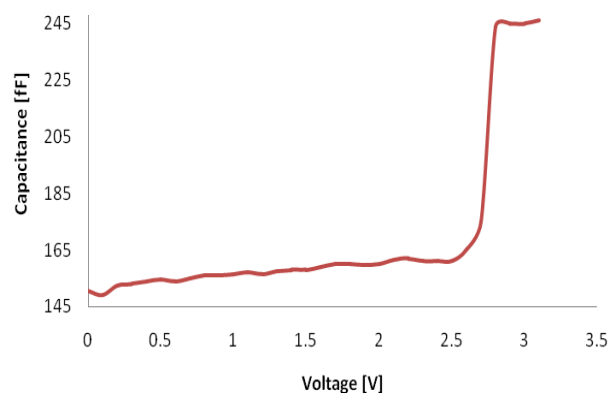


Figure 11. CV measurement

VII. CONCLUSION

The principle, design, fabrication and measurement results of a thin SOI quasi digital accelerometer fabricated were presented. The presented device features quasi-digital output, therefore eliminating the need for analogue signal conditioning circuitry. The use of thin-SOI substrate overcomes the limitations of the Al surface micromachining. The pull-in voltage was 2.7 V. The pull-in time from 0 to 1G was 3.2μs.

ACKNOWLEDGMENT

The authors wish to thank the IC processing group of DIMES for technical assistance.

REFERENCES

- [1] W. C. Tang, Digital Capacitive Accelerometer, US Patent 5353641, 1994.
- [2] H. Yang et al. A novel operation mode for accelerometers, Pacific rim workshop on transducers and micro/nano technologies, July 22-x24, 2002, Xiamen, China, pp.303-306.
- [3] R. E. Ziemer, W. H. Tranter, Principles of communications systems, modulation and noise. Houghton Mifflin Company, 1985.